11ᵗʰ International Conference on Fracture - Turin (Italy), March

WELCOME

PATRONAGE AND AUSPICES

ICF - INTERNATIONAL CONGRESS ON FRACTURE

ICF ORGANIZING COMMITTEE

SCIENTIFIC ADVISORY BOARD

TOPICS

ORGANIZING SECRETARIAT

Dear Colleagues,

On behalf of the Organising Committee of ICF11, I a
International Conference on Fracture, to be held in T
has been organised under the High Patronage of the
the auspices of the Ministry of Infrastructures and Tr
of the National Science Foundation of Italy (CNR), w
worldwide leading Institutions in the fields of Fracture
Integrity, like the International Congress on Fracture
Integrity Society (ESIS), the American Society for Te
Italian Group of Fracture (IGF), the Politecnico di To
have taken the role of host organisations.

The conference is endorsed by a strong scientific programme and by the a
Delegates coming from 52 different Countries. Besides the more traditiona
exciting and new developments such as scaling laws, nanomechanics, sm
tectonics, infrastructure durability, damage and restoration of historical and

12 Plenary Lectures will be delivered by well-known Speakers during the C
Keynote Lectures will be delivered by leading Scientists in the field of Frac
Symposia, whereas nearly 1100 presentations are scheduled to take place
Sessions. This total is obtained by multiplying the 16 parallel sessions by t
conference, and adding four further events in the Auditorium. I would like t
the Organisers of the Special Sessions and Mini-Symposia as well as to th

The Lingotto Conference Centre, selected to host ICF11, is one of the larg
addition, Turin – a very historic and artistic city but also a modern and dyn
best way, as it will be for the Winter Olympic Games one year from now. I
to visit other beautiful places and cities of Italy during your post-conference

I wish you an enjoyable stay in Italy.
Very sincerely yours,

Alberto Carpinteri
ICF11 Chairman

21) HISTORICAL & MONUMENTAL BUILDINGS

5567 - LONG TERM DAMAGE OF HISTORIC MASONRY STRUCTURES
Binda L., Saisi A. (Italy)

5405 - EVOLUTION OF THE CRACK-PATTERN AS A VISIBLE EFFECT OF LONG TERM DAMAGE
Binda L., Anzani A. (Italy)

5413 - PRE-EXISTING DAMAGES AND CHRONOLOGICAL TIME STEP ANALYSES OF HISTORICAL MASONRY BUILDINGS
Calderini C., Lagomarsino S. (Italy)

5523 - MODELLING OF MASONRY CREEP AND DAMAGE
Pina-Henriques J., Lourenço P.B., Krakowiak K.J. (Portugal)

5046 - NUMERICAL EVALUATION OF CRACKING AND CRUSHING IN ANCIENT MASONRY TOWERS
Carpinteri A., Invernizzi S., Lacidogna G. (Italy)

5022 - STRUCTURAL MONITORING AND LIFE-TIME ASSESSMENT OF MEDIEVAL TOWERS
Carpinteri A., Lacidogna G. (Italy)

5707 - CRACK PREDICTION IN MASONRY STRUCTURES
Paradiso M., Tempesta G. (Italy)

5390 - STUDIES ON THE ORIGIN OF DEFORMATION AND DAMAGE IN LONG-SPAN HISTORICAL STRUCTURES
Roca P. (Spain)

5126 - A NUMERICAL MODEL FOR MULTI-LEAF MASONRY
Ramalho M.A. (Brasil), Papa E., Taliercio A., Binda L. (Italy)

5516 - LONG-TERM DAMAGE ON MASONRY TOWERS CASE STUDIES AND INTERVENTION STRATEGIES
Valluzzi M.R., Casarin F., Garbin E., da Porto F., Modena C. (Italy)

MODELLING OF MASONRY CREEP AND DAMAGE

J. Pina-Henriques [1], P.B. Lourenço [1] & K.J. Krakowiak [1]
[1] Department of Civil Engineering, University of Minho, Guimarães, 4800-058, Portugal

ABSTRACT

The problems related to the analysis of ancient constructions are gigantic due to the difficulties in characterizing the geometry, the materials, the sequence of construction, the existing damage and the building processes. A difficult aspect in the repair and strengthening of existing structures is the long-term behaviour of masonry. Safety assessment has been greatly influenced by the collapse of monumental buildings in the last decade, where creep behaviour and creep-fatigue interaction proved to be of relevance for massive masonry walls.

Experimental testing on the creep of regular and rubble ancient masonry together with numerical modelling is currently under investigation by the authors. In a first stage, the research is primarily focused on the monotonic behaviour. This represents a contribution for understanding creep behaviour, providing insight into the basic phenomena that occur in masonry upon increasing loading. The results obtained using a continuous model to represent the masonry components largely overestimated the experimental strength and peak strain. Alternative modelling approaches seem, thus, to be needed and a discontinuous model in which a fictitious micro-structure was given to the components was considered. Clear advantages were shown by this last model. In the present paper, the results obtained using these models are briefly reviewed. The results from the ongoing simulations on the long-term behaviour of masonry assemblages will be presented in the oral communication.

1 INTRODUCTION

Several times during the centuries, and in different sites, the collapse of a tower took place months or even years after a low intensity shake occurred without apparently provoking immediate damage to the structure. In other cases, collapse was not even preceded by a clear change in the loading conditions and the existing damage included only minor diffused cracks. Time-dependent collapse must, thus, be assumed in order to explain such phenomena. Masonry creep depends mainly on factors like state of stress, strength of the material and temperature and humidity conditions, see e.g. Van Zijl [1]. Fatigue actions, like wind and temperature variations, can have a synergetic effect increasing material damage, see e.g. Binda *et al.* [2]. For these reasons, high towers and pillars are the constructions where this phenomenon can more severely occur.

The present research addresses the experimental characterization of the long-term behaviour of ancient masonry together with numerical simulations. The first phase of the research is mainly focused on the behaviour under monotonic loading, as it represents a contribution to understand the basic phenomena involved in compression of masonry assemblages. Several models are being assessed to represent the masonry components. A discussion on the results obtained using a continuous and a discontinuous model is given in the present paper. The results obtained in long-term simulations will be given in the oral communication.

2 EXPERIMENTAL TESTS

Binda *et al.* [3] carried out deformation controlled monotonic tests on masonry prisms with dimensions of $600 \times 500 \times 250$ mm^3, built up with nine courses of $250 \times 120 \times 55$ mm^3 solid soft mud bricks and 10 mm thick mortar joints. Three different types of mortar have been considered and testing aimed at the evaluation of the mechanical compressive properties of the prisms. The masonry components characteristics in terms of the compressive strength f_c, flexural tensile strength f_f, elastic modulus E and coefficient of Poisson ν are given in Table 1. The results obtained for the prisms are given in Table 2. Prisms *P1*, *P2* and *P3* were built with mortars *M1*, *M2* and *M3*, respectively.

Table 1: Mechanical properties of the masonry components.

Component	E [N/mm^2]	ν [-]	f_c [N/mm^2]	f_f [N/mm^2]
Unit	4865	0.09	26.9	4.9
Mortar $M1$	1178	0.06	3.2	0.9
Mortar $M2$	5648	0.09	12.7	3.9
Mortar $M3$	17758	0.12	95.0	15.7

Table 2: Mechanical properties of the masonry prisms.

Prism type	Mortar type	E [N/mm^2]	f_c [N/mm^2]
$P1$	$M1$	1651	11.0
$P2$	$M2$	3833	14.5
$P3$	$M3$	4567	17.8

3 CONTINUOUS MODEL

3.1 Outline of the model

The simulations were carried out resorting to a *basic cell*, i.e., a periodic pattern associated to a frame of reference. For the application envisaged in this section, units and mortar were represented by a structured continuous finite-element mesh. Symmetry conditions have been assumed for in-plane boundaries. In such way, these boundaries remain straight during the analyses and the simulation is carried out as if the specimen was part of a larger portion. Regarding the out-of-plane boundaries, three different approaches were followed: (a) plain stress conditions *PS*, (b) plain strain conditions *PE* and (c) an intermediate state, here named enhanced plain strain *EPE*. This last approach consists on modelling a thin masonry layer with 3D elements, imposing equal displacements in both faces of the layer. Full 3D analyses are unwieldy and were not considered.

For *PS* and *PE* the material behaviour was described by a composite plasticity model with a Drucker-Prager yield criterion in compression and a Rankine yield criterion in tension. The inelastic behaviour exhibits a parabolic hardening/softening diagram in compression and an exponential-type diagram in tension. The material model used in 2D simulations is not available for 3D models and, thus, for *EPE*, a combined model with smeared cracking in tension and Drucker-Prager plasticity in compression had to be used. The models in tension are equivalent, see Lourenço *et al.* [4], but the plasticity based model is numerically more robust.

The simulations were carried out using Diana [5] finite element code. In all simulations, the non-linear equilibrium equations were solved using an incremental-iterative regular Newton-Raphson method, with arc-length control and line-search technique. Yet, severe convergence problems were found, especially in the case of prism *P1*, due to the high ratios between the properties of units and mortar. The model parameters were obtained, whenever possible, from the experimental tests but most of the inelastic parameters were unknown and had to be estimated. A more complete description of this model can be found in Pina-Henriques & Lourenço [6].

3.2 Numerical results

To reproduce correctly the experimental elastic stiffness of masonry prisms, the elastic modulus of the mortar has to be adjusted by inverse fitting. The fact that mortar inside the composite is different from mortar specimens cast separately represents a severe drawback of detailed micro-models and can be explained by mortar laying and curing, see e.g. Lourenço [7]. The diagrams obtained with the experimental mortar stiffness values and with the adjusted values are shown in Figure 1. It can be observed that the *EPE* response is always between the extreme responses obtained with *PS*

and *PE* boundary conditions. For this reason, *EPE* is accepted as the reference solution. It is further noted that the difference between the strength values predicted in *PS* and *PE* conditions increase with larger $f_{c,unit}/f_{c,mortar}$ ratios. This can be explained by the fact that for high ratios between unit and mortar strengths, mortar fails at a very early stage if no out-of-plane confinement is present. Another important point is that the strength and the peak strain for all the three prisms are largely overestimated in the simulations.
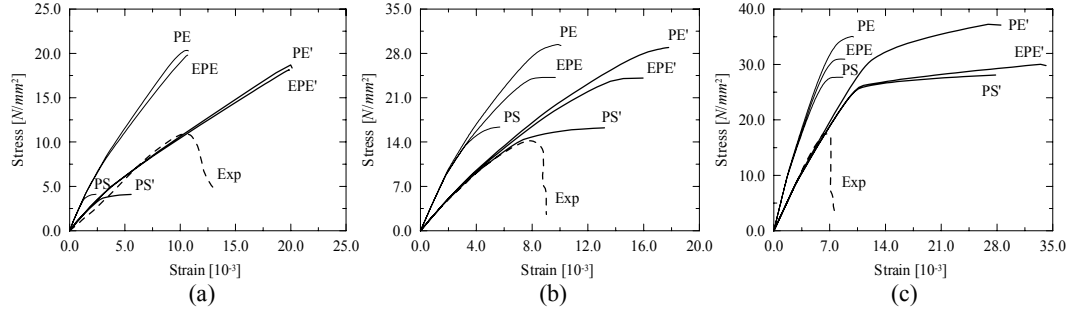

Figure 1: Comparison between the stress-strain diagrams obtained with experimental (*PS*, *PE*, *EPE*) and adjusted (*PS'*, *PE'*, *EPE'*) mortar stiffness values for prisms: (a) *P1*, (b) *P2* and (c) *P3*.

Figure 2 depicts the deformed meshes at failure for prism *P1* in *PS*, *PE* and *EPE* conditions. In addition, the plastic strains contour in the out-of-plane direction is also given in the case of *EPE*. Prism *P1* has been chosen as an example because it has a relatively strong unit and a rather weak mortar as often occurs in ancient masonry. The failure mechanisms obtained depend on the model adopted. This is, of course, physically non-realistic but is a key issue often disregarded. In *PS* conditions, prism *P1* fail due to crushing of the bed joints while in *PE* failure is mainly governed by vertical cracks developing close to the centre of the units and in the head-joints. In *EPE*, the prism fails mainly due to the development of vertical cracks in the centre of the units and in the head-joints while the bed joints show tensile out-of-plane failure.
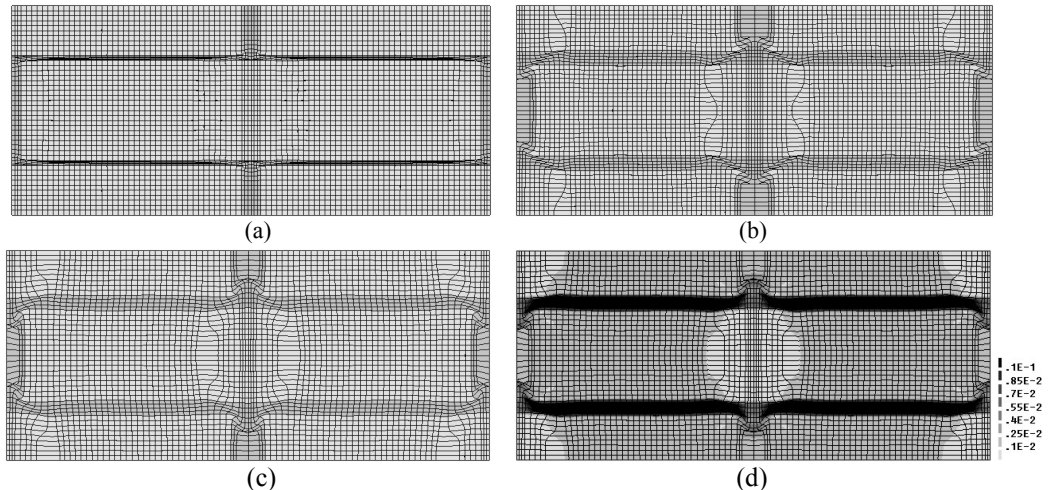

Figure 2: Results obtained for prism *P1*: deformed (incremental) meshes at failure in (a) *PS*, (b) *PE* and (c) *EPE*, and (d) plastic strains in the out-of-plane direction for *EPE*.

Insight on the stress distribution upon increasing loading can be provided by stress diagrams along different sections of the cell, see Figure 3. Severe non-linear behaviour and stress redistribution has been found, with failure not occurring when the maximum stress is attained at a given point of the discretization. As expected, Figure 3a indicates that mortar is heavily triaxially compressed and the units are under combined compression-biaxial tension. A decrease of vertical compressive stresses in the bed-joints is observed near the head-joints due to the low stiffness of the mortar, see Figure 3b. Moreover, in Figure 3c, it is possible to observe that increasing stress concentration develops at the unit edges as load increases and the neighbouring head-joint fails. Also due to increasing damage in the head-joint, the centre of the units exhibit a decrease of compressive vertical stresses as the load increases.
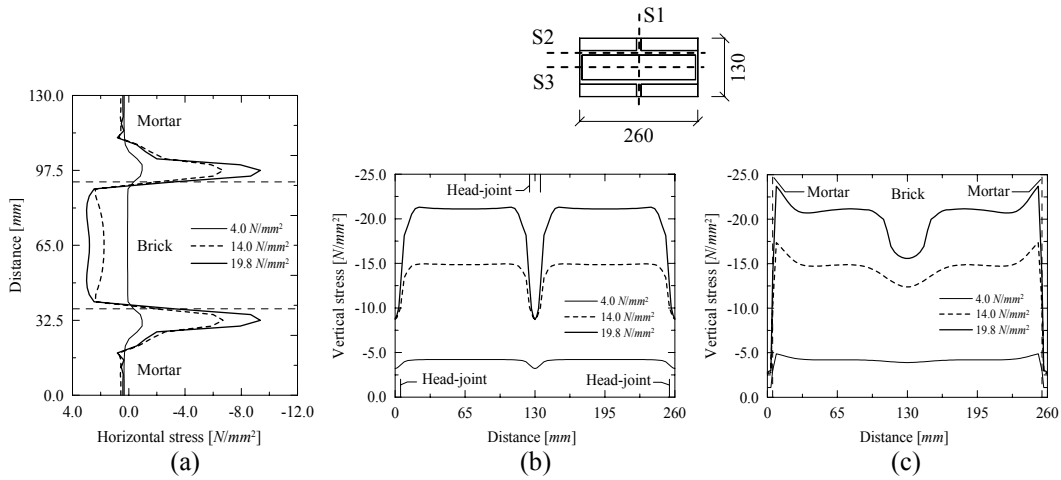

Figure 3: Stress diagrams at increasing load levels for different sections of the cell for prism *P1* (*EPE*): (a) S1, (b) S2 and (c) S3.

4 DISCONTINUOUS INTERFACE MODEL

4.1 Outline of the model

Several advanced computational approaches are currently available to deal with the particulate nature of materials such as soils, rocks, concrete or masonry. Within the most common ones, two main types of analysis can be distinguished: discrete element methods and the finite element method including interface elements *FEM*. The micro-model here proposed is developed on a *FEM* framework, where the discontinuous nature of the masonry components is taken into account by a fictitious micro-structure given to units and mortar. This micro-structure is composed by linear elastic polygons (here named particles) separated by non-linear interface elements, see Figure 4. All the inelastic phenomena occur in the interface elements and the process of fracturing consists of progressive bond-breakage.

The discretization of the continuum into particles is based in the *Voronoi diagram*, according to a specified particle average size and a distortion factor which randomly displaces the particles from their original positions. Material disorder was given to the model by attributing to each particle and to each interface random material parameters following a Gaussian distribution. The mesh was generated by a computer routine written in Visual Basic 6.0. The finite element program adopted was Diana [5,8]. For a comprehensive description of this model the reader is referred to Pina-Henriques & Lourenço [9].
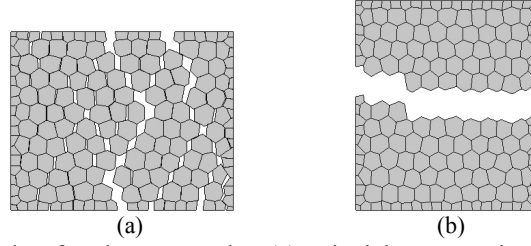
(a)   (b)

Figure 4: Deformed meshes for elements under: (a) uniaxial compression and (b) uniaxial tension.

4.2 Numerical results

Figure 5 shows the numerical diagrams obtained for the basic cell with the interface model. In addition, the diagrams obtained with the continuous model are also illustrated for a better comparison. From the stress-strain diagrams, it is clear that the experimental collapse load is overestimated by the interface model. A similar behaviour was shown by the continuum model although much more satisfactory results have been achieved with the model envisaged in this section, see Table 3. Also in terms of peak strains, the interface model shows clear advantages.
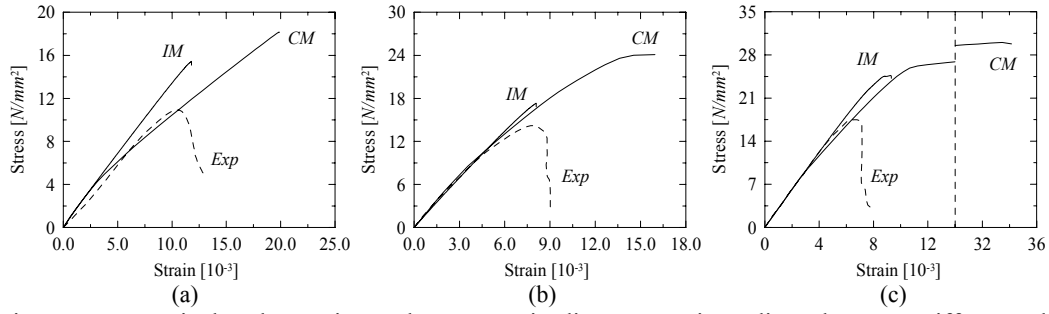

(a)   (b)   (c)

Figure 5: Numerical and experimental stress-strain diagrams, using adjusted mortar stiffness values: (a) prism *P1*, (b) prism *P2* and (c) prism *P3*. In the diagrams, *CM* stands for continuous model, *IM* for interface model and *Exp* for experimental.

Table 3: Experimental and numerical compressive strength values. In brackets are given the strength ratios between the numerical and the experimental values.

	Experimental strength	Continuum model (*EPE*)	Interface model
Prism *P1*	11.0	18.6 (169%)	15.4 (140%)
Prism *P2*	14.5	24.2 (167%)	17.3 (119%)
Prism *P3*	17.8	30.1 (169%)	24.6 (138%)

The numerical failure pattern for prism *P1* is depicted in Figure 6 as an example. The patterns found agree reasonably well with typical compression experimental patterns. For prism *P1*, built with low strength mortar, localized damage developed at the centre of the units while for prisms *P2* and *P3*, which were built with relatively high strength mortar, diffused damage was present. Yet, a certain mesh dependence has been shown by the model, expressed by the development of diagonal damage. It has been shown that this deficiency can be overcome by using high geometrical heterogeneity and by taking the discretization of the continuum to a more refined level. Of course, this has the drawback of increasing dramatically the number of mesh nodes and the computational time. It is also noted that in the case of prism *P1*, the two cracks found at the centre of

the units represent, in reality, a single crack, given that the symmetry conditions adopted and the size and shape of the particles utilized influence the results obtained. Finally, it should be noted that parametric analyses performed with this model showed that shear rather than tensile parameters have a crucial importance in the compressive behaviour of the assemblage.
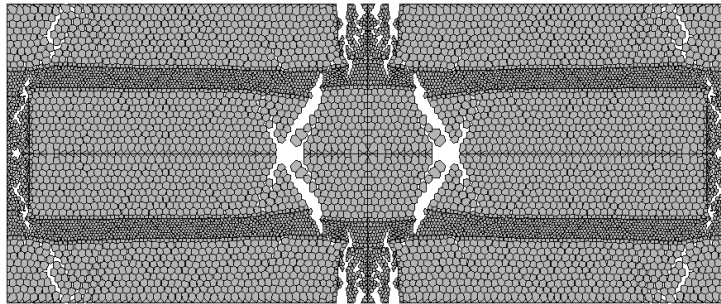

Figure 6: Deformed (incremental) meshes at failure for prism *P1*.

5 CONCLUSIONS

Continuous and discontinuous approaches have been adopted to represent the microstructure of masonry components, attempting to reproduce adequately the experimental behaviour of masonry under monotonic compression. It is noted that the experimental results used for numerical comparison are very demanding with the models, covering a wide range of unit/mortar strength ratios.

The results obtained with short-term loading simulations of masonry prisms allow to conclude that: (a) discontinuous models show clear advantages when compared to continuous models in predicting the compressive behaviour of masonry, including strength and deformability properties and (b) shear parameters rather than tensile parameters play a major role at the micro-level and greatly influence the overall response of masonry loaded in compression.

Tentative suggestions for further work are the assessment of other models developed in a discontinuous framework so that reliable prediction of the masonry monotonic behaviour can be found and modelling of the masonry behaviour under sustained loads.

REFERENCES

[1] Zijl, Van G. Computational modelling of masonry creep and shrinkage. Dissertation, TU Delft, The Netherlands, 2000.

[2] Binda, L., Anzani, A. & Mirabella Roberti, G. Long term behaviour of ancient masonries. *Construction materials – Theory and application*, p. 253-262, 1999.

[3] Binda, L., Fontana, A. & Frigerio, G. Mechanical behaviour of brick masonries derived from unit and mortar characteristics, in: *Proc. 8th IBMaC*, **1**, p. 205-216, 1988.

[4] Lourenço, P.B., Rots, J.G. & Feenstra, P.H. A tensile "Rankine" type orthotropic model for masonry, in: *Proc. 3rd STRUMAS*, p. 167-176, 1995.

[5] Diana Finite Element Code 7.2, TNO Building and Const. Res., The Netherlands, 1999.

[6] Pina-Henriques, J. & Lourenço, P.B. Testing and modelling of masonry creep and damage in uniaxial compression, in Proc. 8th Int. Conf. STREMAH, Halkidiki, Greece, 2003.

[7] Lourenço, P.B. Computational strategies for masonry structures. Dissertation, TU Delft, Delft, The Netherlands, 1996.

[8] Diana Finite Element Code 8.1, TNO Building and Const. Res., The Netherlands, 2003.

[9] Pina-Henriques, J. & Lourenço, P.B. Masonry micro-modelling adopting a discontinuous framework, in Proc. 7th Int. Conf. CST, Lisbon, Portugal, 2004.